Lorentz boosted nucleon-nucleon potential applied to the $^3\vec{\mathrm{H}}\mathrm{e}(\vec{e},e'p)pn$ and $^3\vec{\mathrm{H}}\mathrm{e}(\vec{e},e'n)pp$ processes

J. Golak, R. Skibiński, H. Witała

M. Smoluchowski Institute of Physics,

Jagiellonian University, PL-30059 Kraków, Poland

W. Glöckle

Institut für Theoretische Physik II,

Ruhr Universität Bochum, D-44780 Bochum, Germany

A. Nogga

Forschungszentrum Jülich, IKP (Theorie), D-52425 Jülich, Germany

H. Kamada

Department of Physics, Faculty of Engineering,

Kyushu Institute of Technology, 1-1 Sensuicho,

Tobata, Kitakyushu 804-8550, Japan

(Dated: February 9, 2008)

Abstract

We formulate an approximate relativistic framework for an analysis of the $^3\vec{\mathrm{H}}\mathrm{e}(\vec{e},e'p)pn$ and $^3\vec{\mathrm{H}}\mathrm{e}(\vec{e},e'n)pp$ reactions. Restricting the rescattering series to one term linear in the two-nucleon (2N) t-matrix we incorporate various relativistic features when calculating a nuclear current matrix element. These relativistic ingredients encompass the relativistic ^{3}He wave function based on the concept of the Lorentz boosted nucleon-nucleon potential together with the boosted 2N t-matrix, relativistic kinematics and relativistic single-nucleon current operator. This allows us to estimate the magnitude of relativistic effects not included in the standard nonrelativistic approach.

PACS numbers: 21.45+v,21.10-k,25.10+s,25.20-x

I. INTRODUCTION

Modern three-body calculations allow for a quantitative description of the three-nucleon (3N) system not only in the bound state [1] but also for the continuum states (see for example [2, 3]). This gives the possibility to test our understanding of the three-body system via interactions with external probes. Among many processes which can be listed here, electron scattering on ^{3}He is of special importance [4, 5]. This process serves as a rich source of information about the nucleon form factors [6–9] and important properties of the ^{3}He nucleus [10–12].

Electron induced breakup of ^{3}He involves many components of the dynamical scenario. Among them the initial ^{3}He and final scattering states must be calculated consistently for the same 3N Hamiltonian comprising not only two-nucleon (2N) but also three-nucleon (3N) forces. Consequently, also many-body currents consistent with those forces should be taken into account. We refer the reader to [4] for a detailed discussion of the numerical techniques necessary to perform calculations of this reaction. Currently this can be done only nonrelativistically, which is a major restriction and leads to serious difficulties in interpretation of many experiments performed at high energy and momentum transfers. Due to large differences between the nonrelativistic and relativistic kinematics an analysis of such experiments can not be undertaken within a strictly nonrelativistic framework.

We are not aware of any consistent, relativistic 3N scattering calculation. Also in the present paper we report about a less rigorous approach to the description of the $^3\vec{\mathrm{H}}\mathrm{e}(\vec{e}, e'p)pn$ and $^3\vec{\mathrm{H}}\mathrm{e}(\vec{e}, e'n)pp$ processes. This approach does not include all final state interactions (FSI) among the three outgoing nucleons but restricts the rescattering to only one "spectator" pair of nucleons which is assumed not to take part in the photon absorption. There are definitely kinematical regions where such a reaction mechanism seems to be plausible. Furthermore this approximation was used successfully in the analysis of many experiments (see for example [9, 13]).

We would like to add to this treatment of electron induced breakup of ^{3}He new truly relativistic features. We continue work started in [14], where first steps to extend the Hamiltonian scheme in equal time formulation to 3N scattering were made. To this aim the Lorentz boosted nucleon-nucleon (NN) potential which generates the NN T-matrix in a moving frame via a standard Lippmann-Schwinger equation was calculated and applied to

the 3N bound state problem. In the present paper we show how to obtain the (antisymmetric) 3N relativistic wave function and formulate an approximate framework which can be used as a practical tool for an analysis of experimental results, for example in quasi-elastic reactions at high energy and momentum transfers.

We give the reader a detailed derivation of our formalism in Sec. II. Section III shows our results for the semi-exclusive three-body breakup of ^{3}He. We end with a brief summary in Sec. IV.

II. THEORY

Before we remind the reader of the most important ideas about the Lorentz boosted NN potential, it seems appropriate to start with the well known nonrelativistic concepts.

The nonrelativistic 2N bound state $\mid \psi_b^{(nr)}\rangle$ obeys the equation

$$\mid \psi_b^{(nr)}\rangle = G_0^{(nr)}\, v^{(nr)} \mid \psi_b^{(nr)}\rangle, \tag{1}$$

where $v^{(nr)}$ is the nonrelativistic NN potential and $G_0^{(nr)}$ is the nonrelativistic 2N free propagator. This can be written in the 2N center of mass (c.m.) frame by projecting onto the eigenstate of relative momentum $|\vec{p}>$ ($\vec{p}$ and $-\vec{p}$ are then the individual nucleon momenta)

$$\psi_b^{(nr)}(\vec{p}) = \frac{1}{M_b - 2m - \frac{\vec{p}^{\,2}}{m}} \int d^3p'\, v^{(nr)}(\vec{p},\vec{p}\,')\, \psi_b^{(nr)}(\vec{p}\,'). \tag{2}$$

Here M_b is the 2N bound state rest mass and m is the nucleon mass. The corresponding Lippmann-Schwinger equation

$$t^{(nr)} \;=\; v^{(nr)} \;+\; t^{(nr)}\, G_0^{(nr)}\, v^{(nr)} \tag{3}$$

for the t-matrix $t^{(nr)}$ takes in the momentum space the following form

$$t^{(nr)}(\vec{p},\vec{p}\,') \;=\; v^{(nr)}(\vec{p},\vec{p}\,') \;+\; \int d^3p''\; \frac{t^{(nr)}(\vec{p},\vec{p}\,'')v^{(nr)}(\vec{p}\,'',\vec{p}\,')}{E_{12}^{nr} - \frac{\vec{p}\,''^{\,2}}{m} + i\epsilon}, \tag{4}$$

where E_{12}^{nr} is the nonrelativistic 2N c.m. kinetic energy. The Galilean invariance of the nonrelativistic scenario guarantees that the relative momentum and Eqs.(1)-(4) remain frame independent.

On the other hand, a relativistic NN potential $v^{(rl)}$ defined in the 2N c.m. system appears in the relativistic bound state equation

$$\mid \psi_b^{(rl)}\rangle = G_0^{(rl)}\, v^{(rl)} \mid \psi_b^{(rl)}\rangle, \tag{5}$$

and in the relativistic form of the Lippmann-Schwinger equation

$$t^{(rl)} \,=\, v^{(rl)} \,+\, t^{(rl)}\, G_0^{(rl)}\, v^{(rl)}. \tag{6}$$

In the momentum space spanned by eigenstates of the 2N c.m. relative momentum $\vec{p}$ the Eqs. (5) and (6) can be written as

$$\psi_b^{(rl)}(\vec{p}) = \frac{1}{M_b - \omega(\vec{p})} \int d^3p'\, v^{(rl)}(\vec{p},\vec{p}')\, \psi_b^{(rl)}(\vec{p}\,') \tag{7}$$

and

$$t^{(rl)}(\vec{p},\vec{p}\,') = v^{(rl)}(\vec{p},\vec{p}\,') + \int d^3p''\ \frac{t^{(rl)}(\vec{p},\vec{p}\,'')v(\vec{p}\,'',\vec{p}\,')}{E_{12}^{rl} - \omega(\vec{p}') + i\epsilon}, \tag{8}$$

where

$$\omega(\vec{p}) \equiv 2\sqrt{m^2 + \vec{p}^{\,2}} \tag{9}$$

and the relativistic 2N c.m. energy is denoted by E_{12}^{rl}.

A Lorentz boosted nucleon-nucleon potential $V(\vec{q})$ was introduced in [15] in order to generalize the concept of the relativistic potential for 2N systems with the non-zero total momentum $\vec{q}$. It is formally defined via

$$V(\vec{q}) \,\equiv\, \sqrt{\left[\omega(\vec{p}) + v^{(rl)}\right]^2 \,+\, \vec{q}^{\,2}} \,-\, \sqrt{(\omega(\vec{p}))^2 \,+\, \vec{q}^{\,2}} \tag{10}$$

and by construction fulfills $V(\vec{q} \,=\, 0) \,=\, v^{(rl)}$. The non-trivial task of obtaining matrix elements $V(\vec{p},\vec{p}\,';\vec{q})$ for arbitrary $\vec{q}$ was accomplished in [14].

With use of the boosted potential, the equation for the relativistic 2N bound state moving with the total momentum $\vec{q}$ reads

$$\psi_b^{(rl)}(\vec{p}) = \frac{1}{\sqrt{M_b^2 + \vec{q}^{\,2}} - \sqrt{\omega(\vec{p})^{\,2} + \vec{q}^{\,2}}} \int d^3p'\, V(\vec{p},\vec{p}\,';\,\vec{q})\, \psi_b^{(rl)}(\vec{p}\,'), \tag{11}$$

so the boosted potential allows us to preserve the same structure of the equation as in (2) and (7). Note that $\psi_b^{(rl)}(\vec{p})$ appearing in Eqs. (7) and (11) are identical, i.e. the wave function is represented in a way, which does not depend on $\vec{q}$. This is possible because the relative momenta $\vec{p}$ and $\vec{p}\,'$ in both cases are defined in the 2N c.m. system.

A formalism for treating the relativistic three-body Faddeev equations was introduced in [15, 16]. Since the formal structure of the 3N Hamiltonian

$$H = H_0 + \sum_{i<j} V_{ij}, \tag{12}$$

is the same for relativistic and nonrelativistic approaches, the formal derivation of the Faddeev equations is also the same in both cases [15]. (Note that V_{ij} in 12 is the boosted 2N potential.) Thus the Faddeev component $\mid \Phi\rangle$ of the 3N relativistic wave function $\mid \Psi\rangle$ generated by interaction V in the 2N subsystem obeys

$$\mid \Phi\rangle \;=\; G_0\, T\, P \mid \Phi\rangle, \tag{13}$$

where T is the Lorentz boosted T-matrix generated by potential V, G_0 is the relativistic 3N free propagator and P is a permutation operator which accounts for the fact that we treat nucleons as identical particles. It is given in terms of the transposition P_{ij} interchanging nucleons "i" with "j": $P \equiv P_{12}P_{23} + P_{13}P_{23}$. The wave function $\mid \Psi\rangle$ follows from the Faddeev component via

$$\mid \Psi\rangle = (1 + P) \mid \Phi\rangle. \tag{14}$$

In [15] the boosted T-matrix is constructed from the relativistic 2N t-matrices of Eq.(8) in a quite complicated way. Since we have now the Lorentz boosted potential $V(\vec{q}\,)$ at our disposal, we can obtain the boosted (off-shell) T-matrix directly via the Lippmann-Schwinger equation which, when written in the 3N c.m. system, takes the form

$$T(\vec{p},\vec{p}\,';\,\vec{q}\,) = V(\vec{p},\vec{p}\,';\,\vec{q}\,) \;+\; \int d^3p\,'' \frac{T(\vec{p},\vec{p}\,'';\,\vec{q}\,)\, V(\vec{p}\,'',\vec{p}\,';\,\vec{q}\,)}{E_{3N} - \sqrt{m^2+q^2} \;-\; \sqrt{\omega(\vec{p}\,'')^{\,2} + \vec{q}^{\;2}} + i\epsilon}, \tag{15}$$

where E_{3N} is the total energy of the 3N system and $\vec{q}$ is the momentum of the spectator nucleon ($-\vec{q}$ is then a total momentum of the 2N subsystem). Due to the following observation, Eq. (15) can be solved as easily as Eq. (4). Namely defining

$$f_q(p) \equiv \sqrt{\frac{E_{3N} - \sqrt{m^2+q^2} \;+\; \sqrt{4m^2+4p^2+q^2}}{4\,m}}, \tag{16}$$

$$v(\vec{p},\vec{p}\,';\,\vec{q}\,) \equiv f_q(p)\, V(\vec{p},\vec{p}\,';\,\vec{q}\,)\, f_q(p\,'), \tag{17}$$

$$t(\vec{p},\vec{p}\,';\,\vec{q}\,) \equiv f_q(p)\, T(\vec{p},\vec{p}\,';\,\vec{q}\,)\, f_q(p\,') \tag{18}$$

and

$$p_0^2 \equiv \frac{1}{4}\,\left((E_{3N} - \sqrt{m^2+q^2})^2 - 4m^2 - q^2\right) \tag{19}$$

we arrive at

$$t(\vec{p},\vec{p}\,';\,\vec{q}\,) = v(\vec{p},\vec{p}\,';\,\vec{q}\,) \;+\; \int d^3p''\,\frac{t(\vec{p},\vec{p}\,'';\,\vec{q}\,)\,v(\vec{p}\,'',\vec{p}\,';\,\vec{q}\,)}{\frac{p_0^2}{m}-\frac{\vec{p}\,''^{\,2}}{m}+i\epsilon}. \tag{20}$$

This looks like a nonrelativistic Lippmann-Schwinger equation (4) and can be solved by the same techniques. Once this equation is solved, Eq. (18) is used to get the $T(\vec{p},\vec{p}\,';\,\vec{q}\,)$ matrix elements. Note that p_0^2 in (20) might be in a general case also negative.

As shown in [14] one needs matrix elements of the relativistic potential $v^{(rl)}$ in order to obtain $V(\vec{p}\,',\vec{p};\,\vec{q})$. The boosted potential is then given by the NN bound state wave function and the half-shell NN t-matrices obtained in the 2N c.m. system. The only requirement on $v^{(rl)}$ is that it should describe properly existing 2N data set. It is possible to construct $v^{(rl)}$ directly (see for example [17]) or start with a particular modern nonrelativistic potential $v^{(nr)}$ and apply a scale transformation from [18] to generate a phase equivalent relativistic potential $v^{(rl)}$. This second method was criticized in [19] but nevertheless it remains a possibility for practical calculations. Since the general expression for boosted potential $V(\vec{p},\vec{p}\,';\,\vec{q}\,)$ given in [14] is quite complicated it is desirable to find an approximation simplifying numerical calculations. A simple choice is a restriction to the leading order term in a q/ω and v/ω expansion

$$V(\vec{p},\vec{p}\,';\,\vec{q}\,) \approx v^{(rl)}(\vec{p},\vec{p}\,')\left(1-\frac{\vec{q}^{\,2}}{2\,\omega(\vec{p}\,)\,\omega(\vec{p}\,')}\right), \tag{21}$$

what turned out to be sufficient for a wide range of $\mid \vec{q}\,' \mid$ values [20] (see also [21]). Such an approximation results in a moving deuteron wave function, a binding energy and S- and D-state probabilities very close to the ones for the deuteron at rest.

In a recent paper [22] an alternative way to arrive directly at the boosted NN t-matrix is given. This is without approximation and appears easy to be implemented. Unfortunately, we got aware of that paper only after finishing this study.

We have now all ingredients to write Eq. (13) in the momentum space. It reads in the 3N c.m. system [15, 16]

$$\Phi(\vec{p},\vec{q}\,) = \frac{1}{E_b-\mathcal{E}(\vec{p},\vec{q}\,)}\int d^3q'\,\frac{T_a(\vec{p},\vec{\pi}(\vec{q}\,',-\vec{q}-\vec{q}\,');\vec{q}\,)}{\mathcal{N}(\vec{q}',-\vec{q}-\vec{q}'\,)\,\mathcal{N}(-\vec{q}-\vec{q}',\vec{q}\,)}\,\Phi(\vec{\pi}(-\vec{q}-\vec{q}',\vec{q}\,),\vec{q}\,') \tag{22}$$

where E_b is the 3N binding energy and the index "a" in the boosted T-matrix indicates that it is the properly antisymmetrized operator with respect to exchanges of two interacting nucleons. The vector $\vec{p}$ represents the relative momentum of two interacting nucleons in

their 2N c.m. subsystem, and $\vec{q}$ stands for the momentum of the spectator nucleon ($-\vec{q}$ is the total momentum of the interacting 2N subsystem). The kinetic energy $\mathcal{E}$ is given by

$$\mathcal{E}(\vec{p},\vec{q}) = \sqrt{\omega\left(\vec{p}\right)^2 + \vec{q}^2} + \sqrt{m^2 + \vec{q}^2} - 3m. \tag{23}$$

Let us denote the individual momenta of the three nucleons in their 3N c.m. system by $\vec{p}_i$, their total energies by E_i, and assume that nucleon 1 is the spectator. Then the relation between the momenta $\vec{p}_2$ and $\vec{p}_3$ of two interacting nucleons and their 2N c.m. relative momentum $\vec{p}$, and between spectator momentum $\vec{q}$ and the total momentum $\vec{p}_{23}$ of the interacting 2N subsystem reads

$$\vec{q} = \vec{p}_1 = -\left(\vec{p}_2 + \vec{p}_3\right) \equiv -\vec{p}_{23}, \tag{24}$$

$$\vec{p} \equiv \vec{\pi}\left(\vec{p}_2,\vec{p}_3\right) \equiv \frac{1}{2}\left(\vec{p}_2 - \vec{p}_3\right) - \frac{1}{2}\vec{p}_{23}\left[\frac{E_2 - E_3}{(E_2+E_3) + \sqrt{(E_2+E_3)^2 - \vec{p}_{23}^{\,2}}}\right]. \tag{25}$$

Relations (24) and (25) can be inverted to express the individual momenta $\vec{p}_2$, $\vec{p}_3$ in the 3N c.m. system in terms of the relative momentum $\vec{p}$ of the (23) pair in its 2N c.m. system and its total momentum $\vec{p}_{23}$ in the 3N c.m. system:

$$\vec{p}_2 = \vec{p} + \frac{1}{2}\vec{p}_{23} + \frac{\vec{p}\cdot\vec{p}_{23}}{\left[\omega\left(\vec{p}\right) + \sqrt{\omega\left(\vec{p}\right)^2 + \vec{p}_{23}^{\,2}}\right]\omega\left(\vec{p}\right)}\,\vec{p}_{23}, \tag{26}$$

$$\vec{p}_3 = -\vec{p} + \frac{1}{2}\vec{p}_{23} - \frac{\vec{p}\cdot\vec{p}_{23}}{\left[\omega\left(\vec{p}\right) + \sqrt{\omega\left(\vec{p}\right)^2 + \vec{p}_{23}^{\,2}}\right]\omega\left(\vec{p}\right)}\,\vec{p}_{23}. \tag{27}$$

The two additional factors $\mathcal{N}(\vec{q}\,', -\vec{q} - \vec{q}\,')$ and $\mathcal{N}(-\vec{q} - \vec{q}\,', \vec{q})$ in Eq. (22) which generally can be written as [15]

$$\mathcal{N}(\vec{p}_2,\vec{p}_3) = \left|\frac{\partial(\vec{p}_2,\vec{p}_3)}{\partial(\vec{p},\vec{p}_{23})}\right|^{\frac{1}{2}} = \left(\frac{4E_2E_3}{\sqrt{(E_2+E_3)^2 - \vec{p}_{23}^{\,2}}(E_2+E_3)}\right)^{\frac{1}{2}}, \tag{28}$$

follow from our assumption on normalization of nucleon momentum eigenstates $< \vec{p}_i \mid \vec{p}_i\,' >= \delta(\vec{p}_i - \vec{p}_i\,')$ and the action of the permutation operator P.

In a partial wave representation the relativistic Faddeev Eq. (22) is explicitly given as [15]

$$\phi_\alpha(p,q) \;=\; \frac{1}{E_b - \mathcal{E}(p,q)} \sum_{\alpha'\alpha''} \int_0^\infty dq' q'^2 \int_{-1}^{1} dx \frac{T_{\alpha\alpha'}(p,\pi_1;q')}{{\pi_1}^{l'}}$$

$$\times \frac{G_{\alpha'\alpha''}(q,q',x)}{\mathcal{N}_1(q,q',x)\mathcal{N}_2(q,q',x)} \frac{\phi_{\alpha''}(\pi_2,q')}{{\pi_2}^{l''}}. \tag{29}$$

The index α comprises a set of quantum numbers (channels)

$$\mid \alpha\rangle = \mid (ls)j(\lambda\frac{1}{2})I(jI)J(t\frac{1}{2})T\rangle, \tag{30}$$

where l, s, j and t are the orbital angular momentum, total spin, total angular momentum and total isospin in the two-body subsystem, respectively. The indices λ, I, J, and T stand for the orbital angular momentum, the total angular momentum of the third particle, the total three-body angular momentum, and the total isospin [23]. $G_{\alpha\alpha'}(q,q',x)$ results from matrix element of the permutation operator and is given by (note that there is a misprint in Eq. (B2) of ref. [15])

$$G_{\alpha\alpha'}(q,q',x) = \sum_k P_k(x) \sum_{l_1+l_2=l} \sum_{l_1'+l_2'=l'} p^{l_2+l_2'}\, {p'}^{l_1+l_1'}\, (1+y_1)^{l_2}\, (1+y_2)^{l_1'}\, g_{\alpha\alpha'}^{kl_1l_2l_1'l_2'}. \tag{31}$$

The expressions for π_1, π_2, y_1, y_2, $\mathcal{N}_1(q,q',x)$ and $\mathcal{N}_2(q,q',x)$ as well as other details can be found in [15]. The matrix elements of the permutation operator P that appear in Eqs.(29) and (31) correspond to the form of the permutation operator given in [23]. There also purely geometrical coefficients $g_{\alpha\alpha'}^{kl_1l_2l_1'l_2'}$ are derived (see Eqs. (3.349), (3.352) and (A.19) in that reference). Note that the expressions for the geometrical coefficients are the same in the relativistic and nonrelativistic cases because we neglect the effect of the Wigner spin rotations. This is justified because those effects were found numerically to be of little importance in [20]. Equation (29) was then solved in [14] with the principal result that the relativistic binding energies are smaller by 0.3-0.45 MeV with respect to the nonrelativistic values based on the same 2N potentials.

In many applications the partial wave projected Faddeev components $\phi_\alpha(p,q)$ are not sufficient and we will show now how to obtain the relativistic wave function components $\psi_\alpha(p,q)$ from Eq. (14). To this aim we derive and apply a version of the relativistic operator P "working to the right". As usual it is sufficient to consider only one overlap, for example ${}_1\langle \vec{p}\,\vec{q} \mid \vec{p}\,'\vec{q}\,'\rangle_2$. We restrict ourselves to the 3N c.m. system and express the individual momenta $\vec{p}_1$, $\vec{p}_2$ and $\vec{p}_3$ in terms of $\vec{p}$ and $\vec{q}$ using Eqs. (26) and (27)

$$\vec{p}_1 = \vec{q} \tag{32}$$

$$\vec{p}_2 = \vec{p} - \frac{1}{2}\vec{q} + \frac{\vec{p}\cdot\vec{p}}{\left[\omega\left(\vec{p}\right) + \sqrt{\omega\left(\vec{p}\right)^2 + \vec{q}^{\,2}}\right]\omega\left(\vec{p}\right)}\,\vec{q}, \tag{33}$$

$$\vec{p}_3 = -\vec{p} - \frac{1}{2}\vec{q} - \frac{\vec{p}\cdot\vec{q}}{\left[\omega\left(\vec{p}\right) + \sqrt{\omega\left(\vec{p}\right)^2 + \vec{q}^{\,2}}\right]\omega\left(\vec{p}\right)}\,\vec{q}, \tag{34}$$

Next we calculate the relative momentum of nucleons 3 and 1 in their 2N c.m. frame using Eq. (25)

$$\vec{p}^{\,\prime\prime} \equiv \vec{\pi}\left(\vec{p}_3, \vec{p}_1\right) \equiv \frac{1}{2}\,\left(\vec{p}_3 - \vec{p}_1\right) - \frac{1}{2}\,\vec{p}_{31}\,\left[\frac{E_3 - E_1}{(E_3 + E_1) + \sqrt{(E_3 + E_1)^2 - \vec{p}_{31}^{\,2}}}\right], \tag{35}$$

where $\vec{p}_{31} = \vec{p}_3 + \vec{p}_1 = -\vec{p}_2$. As a consequence ${}_1\langle \vec{p}\,\vec{q} \mid \vec{p}^{\,\prime}\,\vec{q}^{\,\prime}\rangle_2$ becomes

$$\begin{aligned}
{}_1\langle \vec{p}\,\vec{k} \mid \vec{p}^{\,\prime}\,\vec{k}^{\,\prime}\rangle_2 &= \left|\frac{\partial(\vec{p}_2, \vec{p}_3)}{\partial(\vec{p}, \vec{p}_{23})}\right|^{\frac{1}{2}} \left|\frac{\partial(\vec{p}^{\,\prime\prime}, \vec{p}_{31}\,)}{\partial(\vec{p}_3, \vec{p}_1)}\right|^{\frac{1}{2}} \delta^3\left(\vec{p}^{\,\prime} - \vec{p}^{\,\prime\prime}(\vec{p}, \vec{q})\right)\,\delta^3\left(\vec{q}^{\,\prime} - \vec{p}_2(\vec{p}, \vec{q})\right) \qquad (36)\\
&= \left(\frac{4E_2E_3}{(E_2 + E_3)\sqrt{(E_2 + E_3)^2 - \vec{p}_{23}^{\,2}}}\right)^{\frac{1}{2}} \left(\frac{(E_3 + E_1)\sqrt{(E_3 + E_1)^2 - \vec{p}_{31}^{\,2}}}{4E_3E_1}\right)^{\frac{1}{2}}\\
&\qquad \delta^3\left(\vec{p}^{\,\prime} - \vec{p}^{\,\prime\prime}(\vec{p}, \vec{q})\right)\,\delta^3\left(\vec{q}^{\,\prime} - \vec{p}_2(\vec{p}, \vec{q})\right)\\
&\equiv M(\vec{p}, \vec{q})\,\delta^3\left(\vec{p}^{\,\prime} - \vec{p}^{\,\prime\prime}(\vec{p}, \vec{q})\right)\,\delta^3\left(\vec{q}^{\,\prime} - \vec{p}_2(\vec{p}, \vec{q})\right).
\end{aligned}$$

The scalar function $M(\vec{p}, \vec{q})$ actually depends on the magnitudes $\mid \vec{p}\mid$, $\mid \vec{q}\mid$ and the scalar product $x \equiv \hat{p}\cdot\hat{q}$. Again it is easy to recover the nonrelativistic limit of this overlap:

$$M(\vec{p}, \vec{q}) \;\rightarrow\; 1 \tag{37}$$

$$\vec{p}^{\,\prime\prime}(\vec{p}, \vec{q}) \;\rightarrow\; -\frac{1}{2}\vec{p} - \frac{3}{4}\vec{q}, \tag{38}$$

$$\vec{p}_2(\vec{p}, \vec{q}) \;\rightarrow\; \vec{p} - \frac{1}{2}\vec{q}. \tag{39}$$

Having obtained Eq. (36) it is then straightforward to calculate the matrix elements of the permutation operator P in our standard basis [23]

$$\begin{aligned}
&\langle\, p\, q\, \alpha \mid P \mid p'\, q'\, \alpha'\,\rangle \;= \qquad (40)\\
&\int_{-1}^{1} dx\, \frac{\delta(p^{\,\prime} - \tilde{p})}{\tilde{p}^{\,l^{\,\prime}+2}}\, \frac{\delta(q^{\,\prime} - \tilde{q})}{\tilde{q}^{\,\lambda^{\,\prime}+2}}\, \tilde{G}_{\alpha\alpha'}(p, q, x)\, M(p, q, x),
\end{aligned}$$

where

$$\begin{aligned}
\tilde{p} &\equiv \sqrt{\frac{1}{4}p^2(1-g)^2 \;+\; \frac{9}{16}q^2(1+h)^2 \;+\; \frac{3}{4}pqx(1-g)(1+h)}, \qquad (41)\\
\tilde{q} &\equiv \sqrt{p^2 \;+\; \frac{1}{4}q^2(1+2f)^2 \;-\; pqx(1+2f)},
\end{aligned}$$

$$\tilde{G}_{\alpha\alpha'}(p,q,x) = \sum_k P_k(x) \sum_{l'_1+l'_2=l'} \sum_{\lambda'_1+\lambda'_2=\lambda'} p^{\,l'_1+\lambda'_1}\, q^{\,l'_2+\lambda'_2} \\ (1-g)^{l'_1}\,(1+h)^{l'_2}\,(1+2f)^{\lambda'_2}\,\tilde{g}_{\alpha\alpha'}^{kl'_1l'_2\lambda'_1\lambda'_2}, \tag{42}$$

$$f \equiv \frac{-pqx}{\left(2\sqrt{m^2+p^2}+\sqrt{4m^2+4p^2+q^2}\right)2\sqrt{m^2+p^2}}, \tag{43}$$

$$g \equiv \frac{E_3-E_1}{(E_3+E_1)+\sqrt{(E_3+E_1)^2-\vec{p}_{31}^{\,2}}}, \tag{44}$$

and finally

$$h \equiv -\frac{2}{3}f \,+\, \frac{1}{3}g \,+\, \frac{2}{3}fg. \tag{45}$$

The purely geometrical quantity $\tilde{g}_{\alpha\alpha'}^{kl'_1l'_2\lambda'_1\lambda'_2}$ is strictly the same (under the neglection of the Wigner spin rotations) as we use for example in [24]. Consequently, the 3N bound state wave function components can be easily calculated.

We would like to give the reader an example of the difference between the nonrelativistic and relativistic wave function and show the single-nucleon momentum distribution in Fig. 1. We see that differences visible on a logarithmic plot appear only for $q \gtrsim 3$ fm^{-1}. Most important effects are just due to the relativistic kinematics. The approximation given in Eq. (21) does a very good job since the dashed and solid lines nearly overlap. The boost effect is visible for $q \gtrsim 6$ fm^{-1}. The results presented in Fig. 1 and all other results in this paper were obtained with the CD Bonn NN potential [25]. Based on our experience, see for example [26], we expect little sensitivity of our results to the choice of modern high precision NN potential.

III. RESULTS FOR THE $^3\vec{\mathrm{H}}\mathrm{E}(\vec{e},e'\vec{P})pN$ AND $^3\vec{\mathrm{H}}\mathrm{E}(\vec{e},e'\vec{N})pp$ PROCESSES

We will start this section with a brief derivation of the nuclear matrix elements corresponding to Fig. 2. Here we do not take FSI among the three outgoing nucleons fully into account. In the A_1 diagram, which we call the plane wave impulse approximation (PWIA) in this paper, FSI is totally neglected. In the A_2 diagram FSI is restricted only to one pair of nucleons. We will denote the approximation corresponding to the sum of diagrams A_1 and A_2 by FSI23. The laboratory frame coincides with the initial 3N c.m. system so the

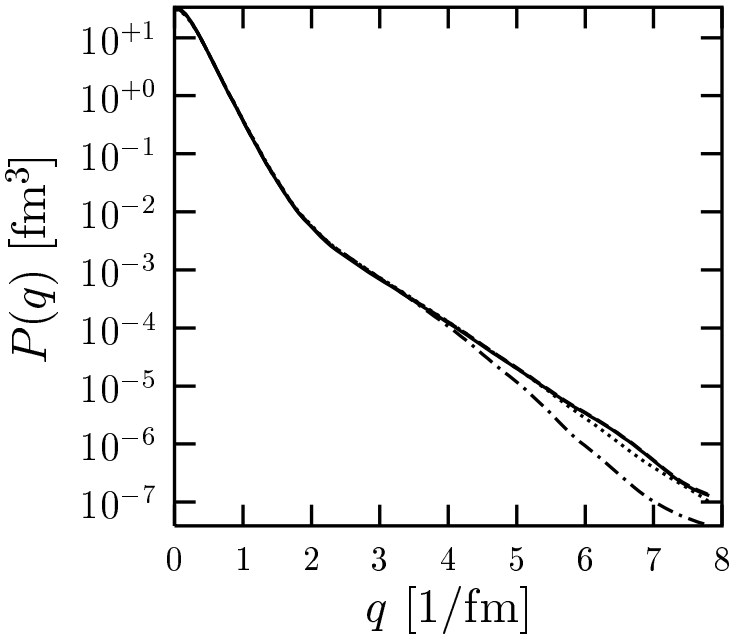

FIG. 1: The single-nucleon momentum distribution for the 3N bound state. The curves correspond to strictly nonrelativistic (dash-dotted), relativistic with no boost effects in the T-matrix (dotted), relativistic with approximate boost effects in the T-matrix according to Eq. (21) (dashed) and fully relativistic calculations (solid).

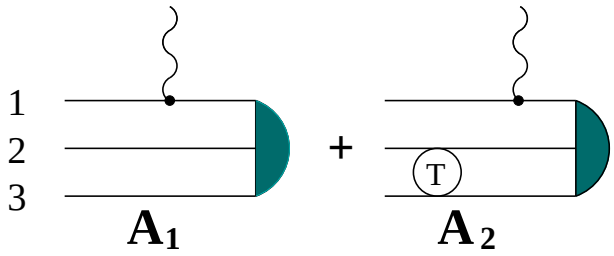

FIG. 2: Diagrammatical representation of the three-body breakup of ^{3}He. The curly lines denote the photon coupling to nucleon 1. The large semi-circles depict the initial ^{3}He bound state. While the diagram A_1 neglects all the final state interactions among the three final nucleons, in the diagram A_2 the boosted scattering operator T acts only in the subsystem (23).

projection of the relativistic wave function on the space of the individual momenta $\vec{p}_i$ reads

$$\langle \vec{p}_1\, \vec{p}_2\, \vec{p}_3 \mid \Psi_b \rangle = \frac{1}{\mathcal{N}(\vec{p}_2, \vec{p}_3\,)}\, \langle \vec{\pi}(\vec{p}_2, \vec{p}_3\,), \vec{p}_1 \mid \Psi_b \rangle. \tag{46}$$

Assuming the action of the single nucleon current operator, the amplitude A_1 takes a very simple form

$$A_1 = \langle \vec{p}_1 m_1 \nu_1 \vec{p}_2 m_2 \nu_2 \vec{p}_3 m_3 \nu_3 \mid j(\vec{Q}, 1) \mid \Psi_b M M_T \rangle, \tag{47}$$

where m_i (ν_i) are spin (isospin) projections of the outgoing nucleons. The spin (isospin) magnetic quantum number of the initial 3N bound state is denoted by M (M_T). ($M_T = \frac{1}{2}$ for the ^{3}He nucleus.) The single nucleon current $j(\vec{Q}, 1)$ acts only on the nucleon 1. One proceeds by inserting single nucleon intermediate states and using (46)

$$\begin{aligned} A_1 = \; & \delta(\vec{p}_1 + \vec{p}_2 + \vec{p}_3 - \vec{Q})\, \textstyle\sum_{m_1'}\, j(\vec{p}_1, \vec{p}_1 - \vec{Q}; m_1, m_1'; \nu_1) \\ & \langle \vec{p}\, \vec{q}\, m_1' m_2 m_3 \nu_1 \nu_2 \nu_3 \mid \Psi_b M M_T \rangle\; \tfrac{1}{\mathcal{N}(\vec{p}_2, \vec{p}_3)}, \end{aligned} \tag{48}$$

where $\vec{p} \equiv \vec{\pi}(\vec{p}_2, \vec{p}_3)$, and $\vec{q} \equiv \vec{p}_1 - \vec{Q}$. Finally we use the partial wave decomposition of the bound state in the basis $\mid pq\alpha \rangle$ and arrive at

$$\begin{aligned} A_1 = {} & \delta(\vec{p}_1 + \vec{p}_2 + \vec{p}_3 - \vec{Q})\; \delta_{\nu_1+\nu_2+\nu_3, M_T} \\ & \frac{1}{N(\vec{p}_2, \vec{p}_3)}\; \sum_{m_1'} j(\vec{p}_1, \vec{p}_1 - \vec{Q}; m_1, m_1'; \nu_1) \\ & \sum_{\alpha'}\; \sum_{\mu'}\; C(j', I', \frac{1}{2}; \mu', M - \mu', M)\; C(l', s', j'; \mu' - m_2 - m_3, m_2 + m_3, \mu') \\ & C(\frac{1}{2}, \frac{1}{2}, s'; m_2, m_3, m_2 + m_3)\; C(\lambda', \frac{1}{2}, I'; M - \mu' - m_1', m_1', M - \mu') \\ & C(t', \frac{1}{2}, \frac{1}{2}; \nu_2 + \nu_3, \nu_1, \nu_1 + \nu_2 + \nu_3)\; C(\frac{1}{2}, \frac{1}{2}, t'; \nu_2, \nu_3, \nu_2 + \nu_3) \\ & Y_{l', \mu' - m_2 - m_3}(\hat{p})\; Y_{\lambda', M - \mu' - m_1'}(\hat{q})\; \langle pq\alpha' \mid \Psi_b \rangle. \end{aligned} \tag{49}$$

The amplitude A_2 additionally contains the free 3N propagator G_0 and the (half-shell) boosted scattering operator T acting in the (23) subsystem

$$\begin{aligned} A_2 = {} & \langle \vec{p}_1 m_1 \nu_1 \vec{p}_2 m_2 \nu_2 \vec{p}_3 m_3 \nu_3 \mid T\, G_0\, j(\vec{Q}, 1) \mid \Psi_b M M_T \rangle \\ = {} & \delta(\vec{p}_1 + \vec{p}_2 + \vec{p}_3 - \vec{Q})\; \delta_{\nu_1+\nu_2+\nu_3, M_T}\; \delta_{\nu_1, \nu_1'}\; \frac{1}{\mathcal{N}(\vec{p}_2, \vec{p}_3)} \\ & \sum_{m_1'} j(\vec{p}_1, \vec{p}_1 - \vec{Q}; m_1, m_1'; \nu_1) \\ & \int d\vec{p}\,' \sum_{m_2', m_3'}\; \sum_{\nu_2', \nu_3'}\; \delta_{\nu_2+\nu_3, \nu_2'+\nu_3'} \end{aligned}$$

$$\langle \vec{p} m_2 m_3 \nu_2 \nu_3 \mid T(\vec{p}_2 + \vec{p}_3) \mid \vec{p}\,' m_2' m_3' \nu_2' \nu_3' \rangle$$
$$\frac{1}{E_2 + E_3 \; - \; \sqrt{4m^2 + 4\vec{p}\,'^{\,2} + (\vec{Q} - \vec{p}_1)^{\;2}} \; + i\epsilon}$$
$$\langle \vec{p}\,' \vec{q} m_1' m_2' m_3' \nu_1' \nu_2' \nu_3' \mid \Psi_b M M_T \rangle. \tag{50}$$

In the final step both the bound state wave function and the T-matrix are given in the partial wave basis, which yields

$$\begin{aligned} A_2 = \delta(\vec{p}_1 + \vec{p}_2 + \vec{p}_3 - \vec{Q}) \; \delta_{\nu_1+\nu_2+\nu_3, M_T} \; \frac{1}{\mathcal{N}(\vec{p}_2, \vec{p}_3)} \\ \sum_{m_1'} j(\vec{p}_1, \vec{p}_1 - \vec{Q}; m_1, m_1'; \nu_1) \\ \sum_{lsj\mu t} \; C(l, s, j; \mu - m_2 - m_3, m_2 + m_3, \mu) \; C(\frac{1}{2}, \frac{1}{2}, s; m_2, m_3, m_2 + m_3) \\ C(t, \frac{1}{2}, \frac{1}{2}; \nu_2 + \nu_3, \nu_1, \nu_1 + \nu_2 + \nu_3) \; C(\frac{1}{2}, \frac{1}{2}, t; \nu_2, \nu_3, \nu_2 + \nu_3) \\ Y_{l, \mu - m_2 - m_3}(\hat{p}) \; \sum_{\bar{l}} \sum_{\alpha'} \delta_{l\bar{l}} \, \delta_{s's} \, \delta_{j'j} \, \delta_{t't} \, C(j, I', \frac{1}{2}; \mu, M - \mu, M) \\ C(\lambda', \frac{1}{2}, I'; M - \mu - m_1', m_1', M - \mu) \; Y_{\lambda', M - \mu - m_1'}(\hat{q}) \\ \int dp' \, p'^{\;2} \; \langle p(ls)jt \mid T(\vec{Q} - \vec{p}_1) \mid p'(l's')jt \rangle \; \langle p' q \alpha' \mid \Psi_b \rangle \\ \frac{1}{E_2 + E_3 \; - \; \sqrt{4m^2 + 4\vec{p}\,'^{\,2} + (\vec{Q} - \vec{p}_1)^{\;2}} + i\epsilon}. \end{aligned} \tag{51}$$

The single nucleon current matrix elements $j(\vec{p}_1, \vec{p}_1{}'; m_1, m_1'; \nu_1)$ (ν_1 decides whether the photon couples to a proton or to a neutron) are taken completely relativistically, i.e.,

$$\begin{aligned} j(\vec{p}, \vec{p}\,'; m_1, m_1') \equiv j^\mu(\vec{p}, \vec{p}\,'; m_1, m_1') \; = \sqrt{\frac{m}{\sqrt{m^2 + p^2}}} \; \sqrt{\frac{m}{\sqrt{m^2 + p'^{\,2}}}} \\ \bar{u}(p m_1) \, (F_1 \gamma^\mu + i F_2 \sigma^{\mu\nu} (p - p')_\nu) \, u(p' m_1'), \end{aligned} \tag{52}$$

where u are Dirac spinors. $F_1(p' - p)^2)$ and $F_2(p' - p)^2)$ are Pauli and Dirac nucleon form factors, respectively. In this paper we used the Höhler parametrization for the nucleon electromagnetic form factors [27].

In this section the results for the three-body breakup will be discussed. We assume the reference frame for which the three-momentum transfer $\vec{Q} \equiv \vec{k} - \vec{k}\,'$ is parallel to $\hat{z}$, $\hat{y} \equiv \frac{\vec{k}\,' \times \vec{k}}{|\vec{k}\,' \times \vec{k}|}$, and $\hat{x} = \hat{y} \times \hat{z}$. Here $\vec{k}$ and $\vec{k}\,'$ are the initial and final electron momenta. The exclusive cross section for the $e + {}^3\mathrm{He} \rightarrow e' + p + p + n$ reaction has the form [28]

$$d\sigma(\vec{S}, h) \;\; = \;\; \sigma_{\mathrm{Mott}} \; \{ \, (v_L W_L + v_T W_T + v_{TT} W_{TT} + v_{TL} W_{TL})$$

$$+ \; h \; (v_{T'} W_{T'} + v_{TL'} W_{TL'}) \; \} \; \delta \left(k + m_{^3\mathrm{He}} - k' - E_1 - E_2 - E_3\right)$$
$$\delta \left(\vec{k} - \vec{k}' - \vec{p}_1 - \vec{p}_2 - \vec{p}_3\right) \; d^3\vec{k}' \, d^3\vec{p}_1 \, d^3\vec{p}_2 \, d^3\vec{p}_3, \tag{53}$$

where σ_{Mott} and all v_i are analytically given kinematical factors, h is the helicity of the incoming electron and $\vec{S}$ represents the initial ^{3}He spin direction. The electron mass is neglected and $m_{^3\mathrm{He}}$ denotes the ^{3}He mass. The response functions W_i, which contain the whole dynamical information, are constructed from the nuclear current matrix elements taken between the initial bound state and the final scattering state. Using Eq. (53) three observables which we consider in this paper can be easily constructed. The first one is the unpolarized sixfold differential cross section

$$\frac{d^6\sigma}{dk' \, d\hat{k}' \, dE_1 \, d\hat{p}_1} \; = \; \frac{1}{2} \sum_{m_S} \sum_{m_1, m_2, m_3} \mathcal{C} \int d\hat{p} \, \mathcal{J} \, p_1 E_1 \, \frac{1}{4}(E_2 + E_3) \, p$$
$$\sigma_{\mathrm{Mott}} \; (v_L W_L + v_T W_T + v_{TT} W_{TT} + v_{TL} W_{TL}) \; , \tag{54}$$

where m_S, m_1, m_2, m_3 are spin projections of the initial ^{3}He and of the three outgoing nucleons. The relativistic relative momentum $\vec{p} \equiv p\hat{p}$ is defined in Eq. (25). The additional factor $\mathcal{C} = \frac{1}{2}$ is necessary only if the observed particle is a neutron (the two not detected particles are then identical). Note that we changed variables according to [15]

$$d^3\vec{p}_1 \, d^3\vec{p}_2 \, d^3\vec{p}_3 \; = \; \mathcal{J} \, d^3\vec{p}_1 \, d^3\vec{p}_{23} \, d^3\vec{p}, \tag{55}$$

in order to simplify integrations over the unobserved parameters of the final 3N system. The kinematical factors in Eq. (54) simplify significantly in the nonrelativistic limit

$$\vec{p} \to \frac{1}{2} \, (\vec{p}_2 - \vec{p}_3 \,)$$
$$E_i \to m$$
$$\mathcal{J} \to 1 \tag{56}$$

The second and third observables we investigate here are special cases of the helicity asymmetry $A(\vec{S})$

$$A(\vec{S} \,) \equiv \frac{\sigma(\vec{S}, h = +1) - \sigma(\vec{S}, h = -1)}{\sigma(\vec{S}, h = +1) + \sigma(\vec{S}, h = -1)}, \tag{57}$$

under the same kinematical conditions as the unpolarized cross section in Eq. (54) and obtained from the corresponding polarized semi-exclusive cross sections $\sigma(\vec{S}, h)$. We consider

$A_\parallel$ for $\vec{S} \parallel \hat{z}$ and $A_\perp$ for $\vec{S} \parallel \hat{x}$. Further we stick to the so-called parallel kinematics, for which the finally observed nucleon is ejected parallel to $\vec{Q}$. In this case $W_{TT} = W_{TL} = 0$. This choice of kinematical conditions is optimal for the FSI23 approximation. We can expect that under these kinematics, at least for high energies, the reaction mechanism is dominated by the processes depicted in Fig. 2.

Our nonrelativistic framework [4] allows us to calculate the initial ^{3}He and final scattering states consistently using any 3N realistic Hamiltonian and including also many-body current operators. There is no such relativistic dynamical framework available at the moment and in this paper we would like to study what are the different effects when some nonrelativistic elements are replaced by their relativistic counterparts. We focus on the approximation depicted in Fig. 2 and calculate the matrix elements corresponding to diagrams A_1 and A_2, first strictly nonrelativistically, secondly using a mixed approach [13] with the nonrelativistic t-matrix and wave functions but employing relativistic kinematics and the relativistic single nucleon current operator. Finally, we use consistently the relativistic 3N bound state, kinematics, the boosted T-matrix and the relativistic single nucleon current operator, as described in Sec. II.

We chose eight electron kinematics (see Fig. 3 and Table I), characterized by the same electron beam energy (E=2000 MeV) and different values of the energy (ω) and momentum ($Q =\mid \vec{Q} \mid$) transfers. For some of them full inclusion of FSI is possible within our nonrelativistic framework, since the 3N c.m. energy does not allow for pion production. In that case we always used the nonrelativistic current operator. We will thus check to what extent the FSI23 approximation might be sufficient and then concentrate more on different relativistic effects within this simplified relativistic framework. For more detailed discussion of the validity of the FSI23 approximation see [29].

The kinematics $k1$-$k6$ are chosen along the quasi-elastic scattering line. The additional kinematics $k7$ and $k8$ are chosen above and below the quasi-elastic line in order to identify differences with respect to the kinematics that belong to the quasi-elastic scattering group.

In the first two figures (4 and 5) we show the parallel helicity asymmetry $A_\parallel$ both for the neutron and proton knockout. In most cases the FSI23 approximation is not sufficient, i.e. the nonrelativistic FSI23 curve lies far away from the nonrelativistic prediction taking FSI fully into account. The latter reveals very often much a more complicated behavior contrary to the rather simple shapes of the FSI23 predictions. This FSI23 approximation turns out

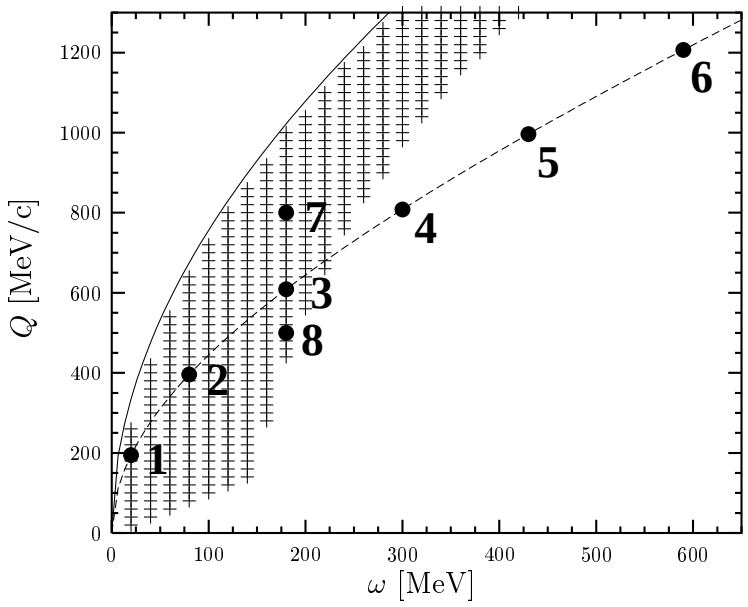

FIG. 3: Eight electron kinematics ((ω, Q) points) considered in the present paper are marked as full circles. The shaded area shows the (ω, Q) points for which the 3N c.m. kinetic energy is smaller than the pion mass. The solid lined corresponds to elastic electron scattering on ^{3}He and the dashed line to the quasi-free scattering condition (scattering on a free nucleon).

electron kinematics	θ_e [deg]	E' [MeV]	ω [MeV]	Q [MeV/c]	$E^{\rm 3N}_{\rm c.m.}$(rel) [MeV]	$E^{\rm 3N}_{\rm c.m.}$(nrl) [MeV]
k1	5.6	1980	20	194.8	5.6	5.5
k2	11.4	1920	80	395.8	45.0	44.5
k3	17.5	1820	180	608.6	109.7	106.5
k4	23.5	1700	300	808.3	185.4	176.3
k5	29.4	1570	430	996.2	265.3	246.1
k6	36.5	1410	590	1206.7	360.9	323.8
k7	23.6	1820	180	800.0	63.2	58.7
k8	14.0	1820	180	500.0	130.2	127.9

TABLE I: Parameters of the eight electron kinematics studied in this paper: the electron scattering angle θ_e, the outgoing electron energy E', the energy transfer ω, the magnitude of the three-momentum transfer Q, the relativistic ($E^{\rm 3N}_{\rm c.m.}$(rel)) and nonrelativistic ($E^{\rm 3N}_{\rm c.m.}$(nrl)) kinetic c.m. 3N energies.

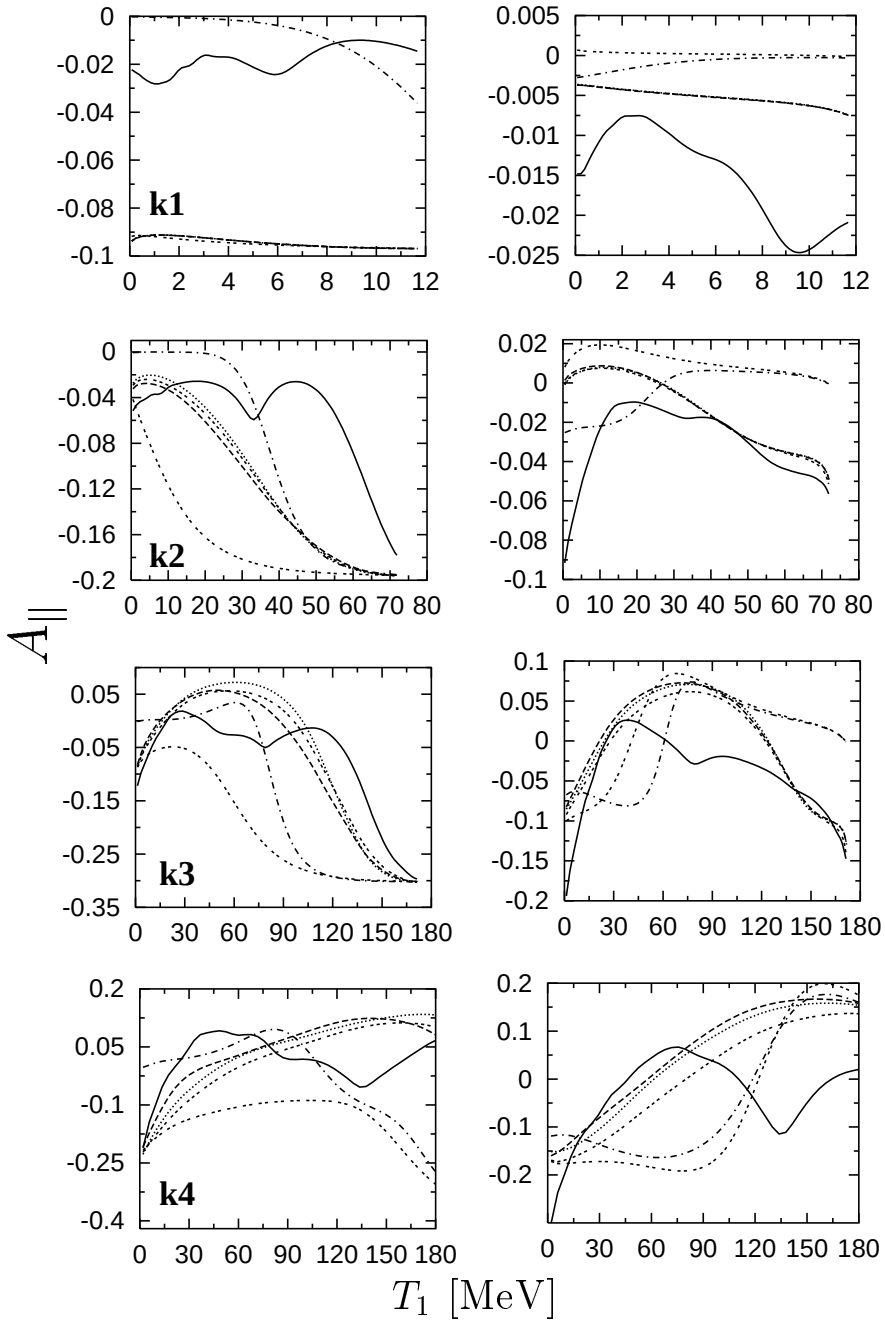

FIG. 4: The parallel asymmetry $A_{\parallel}$ for the neutron (left panel) and proton (right panel) ejection in the virtual photon direction as a function of the emitted nucleon kinetic energy $T_1 \equiv E_1 - m$ for the first four electron kinematics from Table I. The double dashed line shows the nonrelativistic PWIA prediction and the dash-dotted line the nonrelativistic symmetrized PWIA (PWIAS) prediction. Further we show the strictly nonrelativistic FSI23 results (triple dashed line), the FSI23 predictions with some relativistic features as described in the text (dotted line), and the consistent relativistic FSI23 results (dashed line). Finally the prediction with full inclusion of FSI is represented by the solid line.

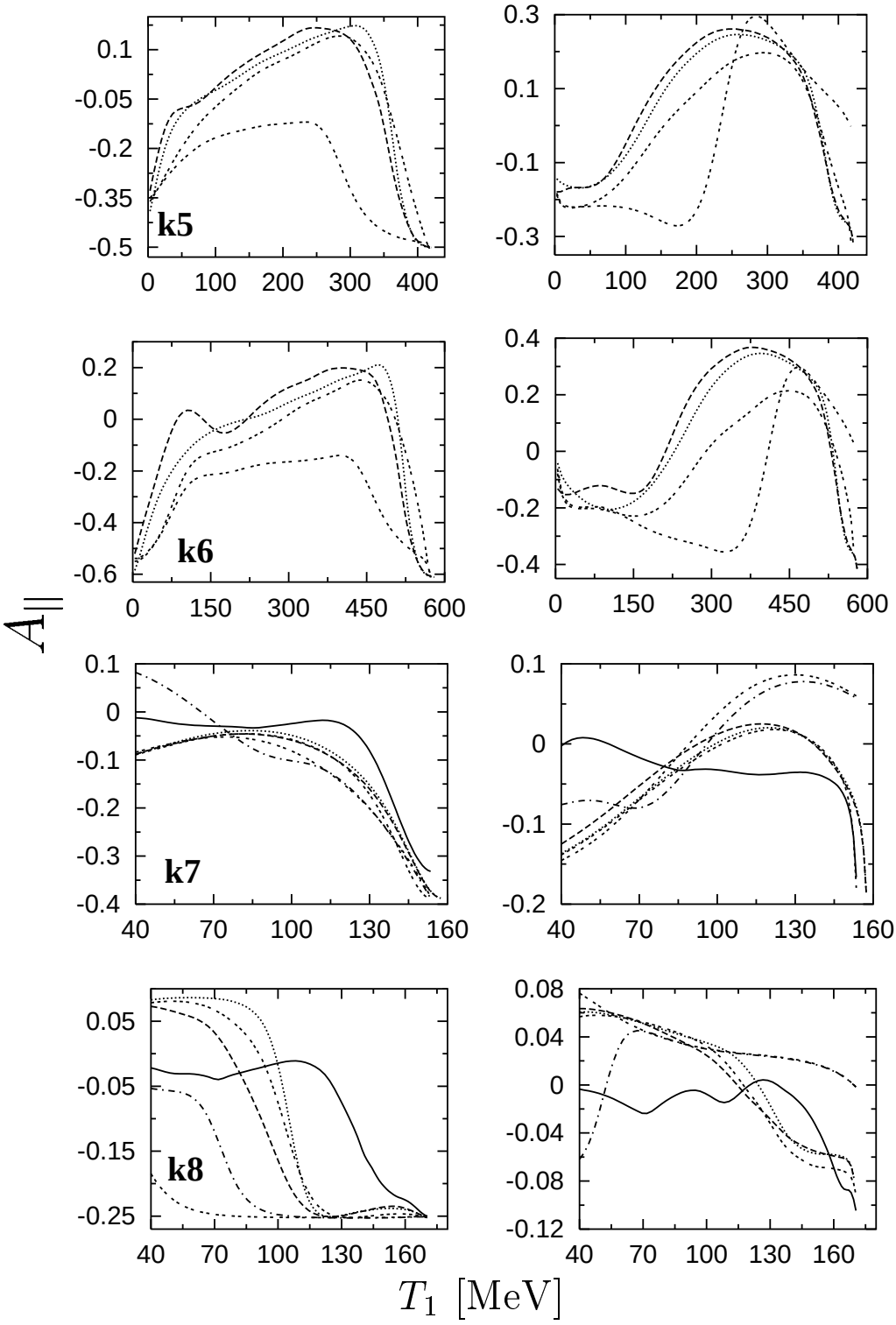

FIG. 5: The same as in Fig. 4 for the remaining four electron kinematics from Table I. The PWIAS prediction and the one with full FSI are missing for the $k5$ and $k6$ kinematics.

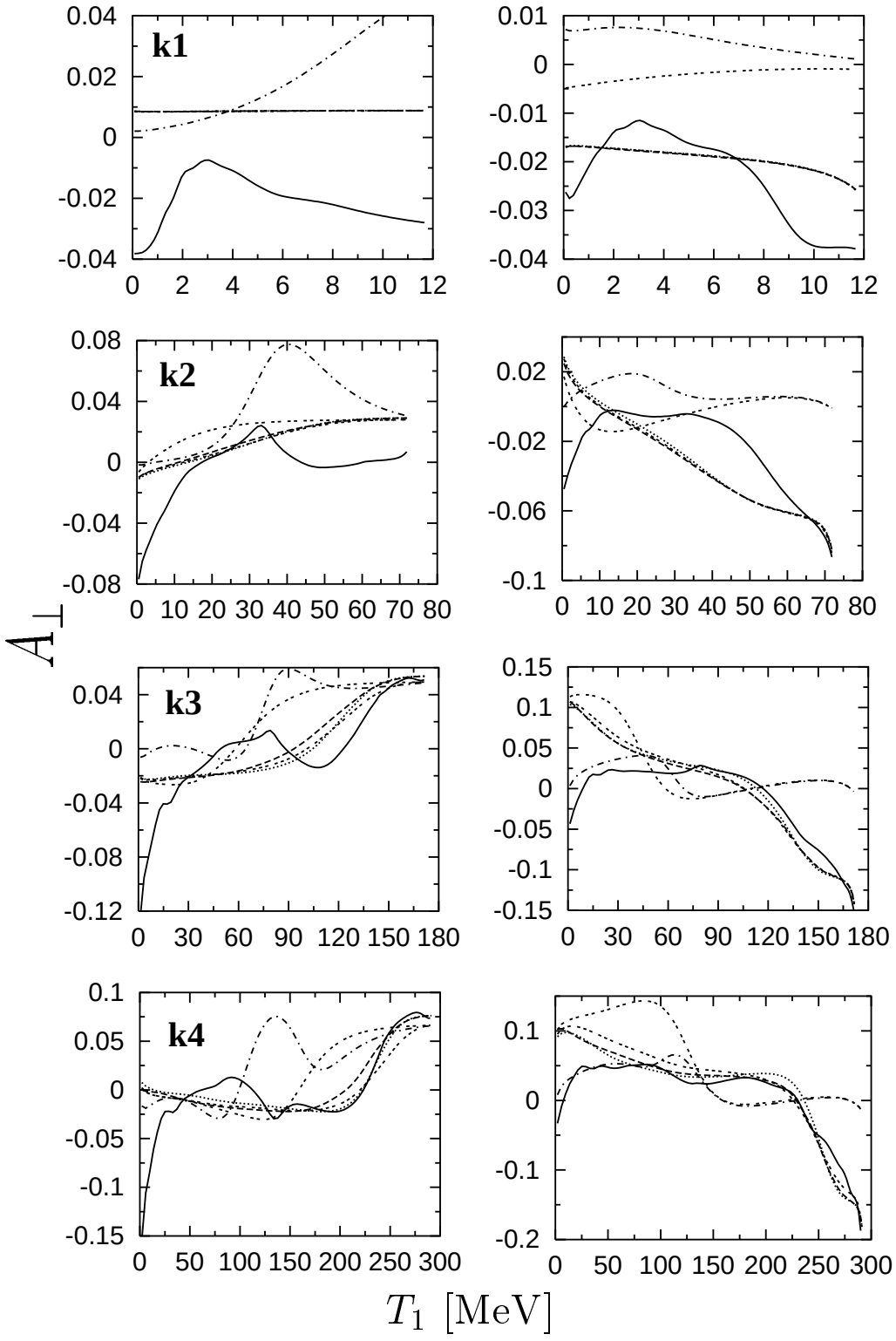

FIG. 6: The same as in Fig. 4 for the perpendicular asymmetry $A_\perp$.

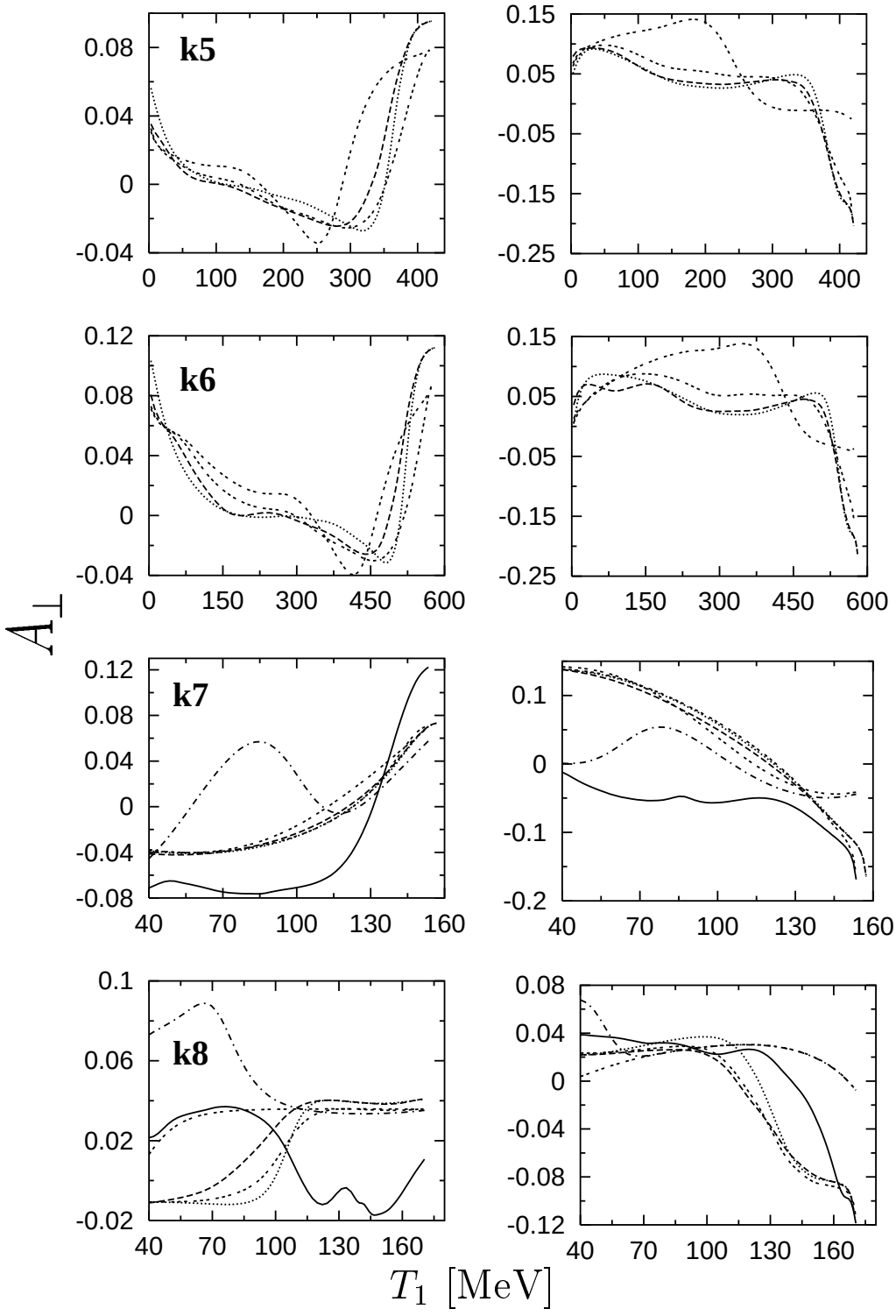

FIG. 7: The same as in Fig. 6 for the remaining four electron kinematics from Table I. The PWIAS prediction and the one with full FSI are missing for the $k5$ and $k6$ kinematics.

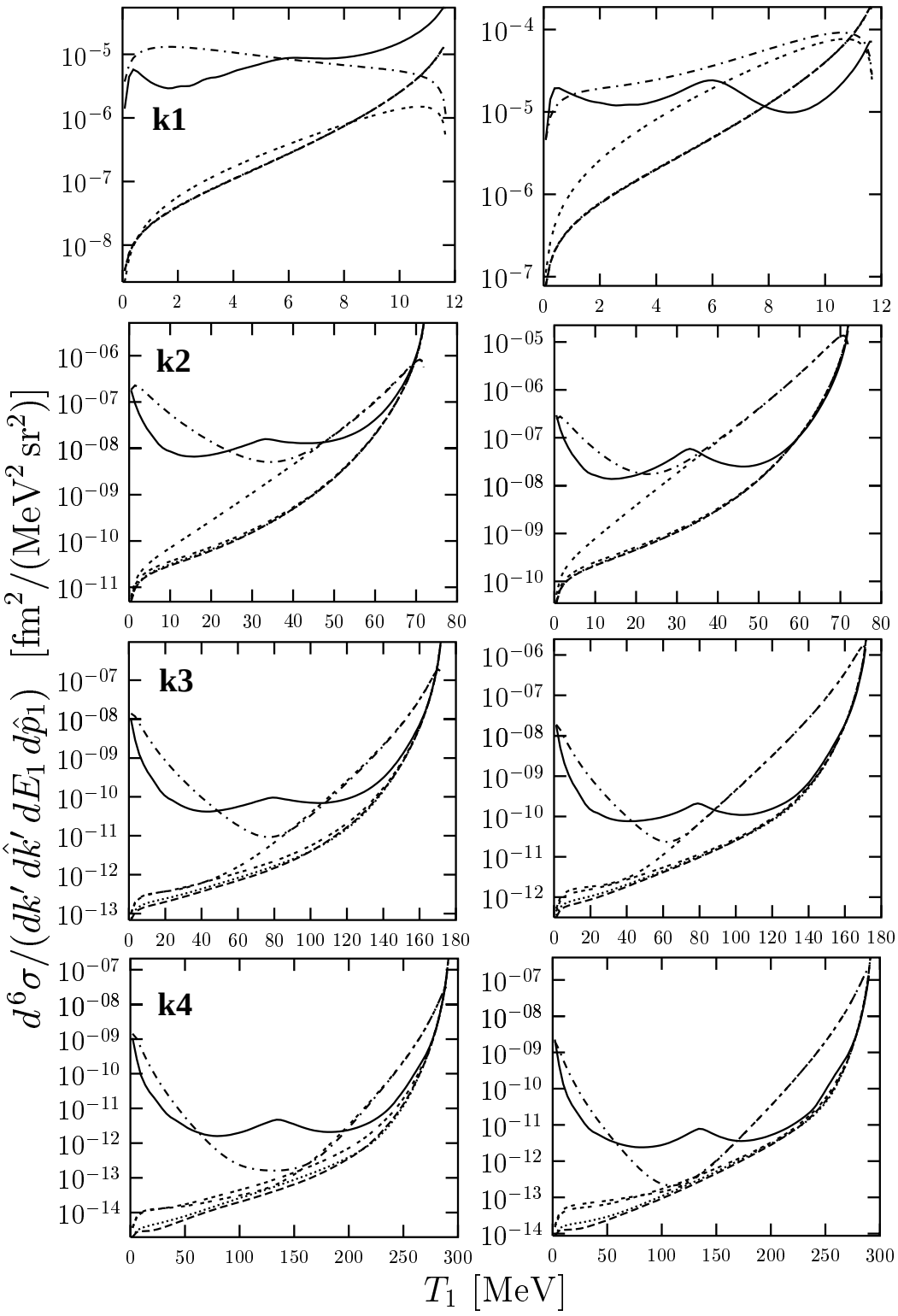

FIG. 8: The same as in Fig. 4 for the sixfold differential cross section.

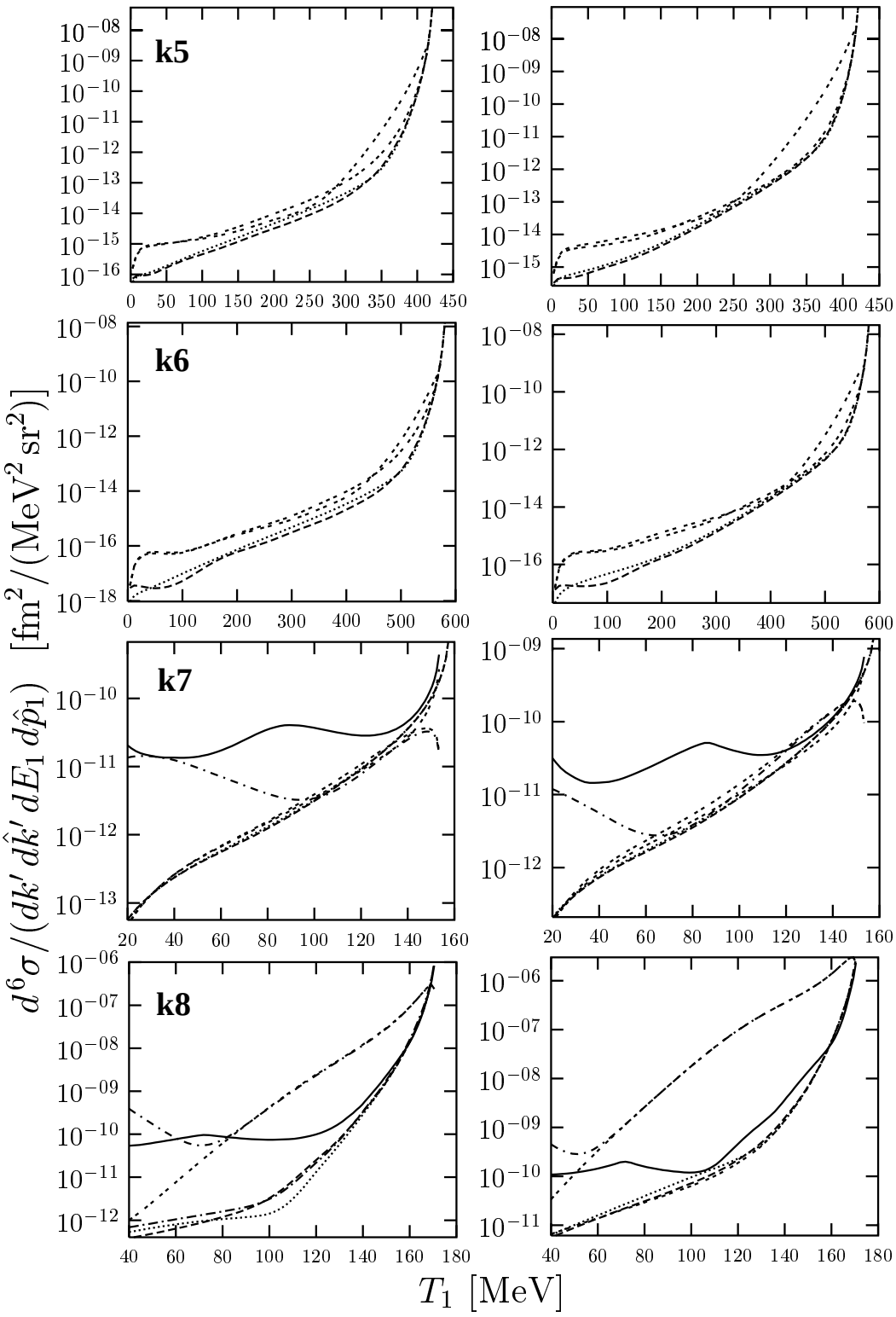

FIG. 9: The same as in Fig. 8 for the remaining four electron kinematics from Table I. The PWIAS prediction and the one with full FSI are missing for the $k5$ and $k6$ kinematics.

to be satisfactory (however not always) only at the upper end of the energy spectrum for higher magnitudes of the three-momentum transfers. It is interesting to notice that the contribution from the A_2 diagram is very small for the k_1 kinematics in the neutron case. Here the PWIA and all FSI23 curves overlap. That does not mean, however, that all FSI is negligible in this case. Already the symmetrization in the plane wave predictions changes the picture significantly and the results with full inclusion of FSI are still very different.

The relativistic effects (the spread among the three FSI23 predictions) are generally most evident not for the maximal energy of the ejected nucleon, where the (23) subsystem c.m. energy is very small, but rather in the middle of the nucleon energy range. Generally, the mixed approach to the FSI23 calculation is closer to the relativistic result than its fully nonrelativistic partner. Especially for the $k7$ kinematics the difference between the relativistically and nonrelativistically calculated maximal energy of the knocked out nucleon is clearly visible. For the neutron knockout at the $k3$ and $k4$ kinematics the asymmetries tend to reach specific values which depend only on the neutron magnetic form factors and trivial kinematic factors. This corresponds very closely to electron scattering on a free, fully polarized neutron at rest and was suggested as a way to access the important neutron property, since there is no free neutron target in nature. Note the big differences between the results for the $k3$, $k7$ and $k8$ kinematics which all belong to the same energy transfer ω but have different magnitude Q of the three momentum transfer.

These differences are even more true for the perpendicular helicity asymmetry $A_\perp$ displayed in Figs. 6 and 7. For this observable, especially in the case of the neutron knockout, FSI23 predictions come close to the results fully employing FSI only for the $k3$ kinematics, which lies on the quasi-elastic scattering curve. The FSI23 predictions lie lower ($k7$) or higher ($k8$) than the results based on the more complete dynamical model. Also for this asymmetry the PWIA and FSI23 predictions take very simple shapes at the first two kinematics, while the full inclusion of FSI leads to more complicated structures. The perpendicular asymmetry for the neutron knockout process is very sensitive to the neutron electric form factor so also in this case the values for the maximal neutron energies, especially at the $k3$ and $k4$ kinematics, are determined predominantly by the neutron electric form factor values. This explains why in the neutron case the parallel asymmetry is much bigger than the perpendicular one.

For the $k5$ and $k6$ kinematics there is a clear gap between the pure nonrelativistic FSI23

result and the predictions employing relativistic kinematics and the relativistic current operator. This is partly due to the arguments of the electromagnetic form factors, which differ for these two approaches. In the nonrelativistic case we simply take $\omega^2 - \vec{Q}^{\,2}$ which does not correspond to the true four-momentum transfer felt by the nucleon. In the relativistic case we (exactly) account for the four momentum transferred to the nucleon using the following form

$$\left(\sqrt{m^2 + \left(\vec{p} + \vec{Q}\right)^2} - \sqrt{m^2 + \vec{p}^{\,2}}\right)^2 - \vec{Q}^{\,2}, \tag{58}$$

where $\vec{p}$ is the nucleon momentum prior to photon absorption.

Finally, in Figs. 8 and 9, we show the six fold differential cross sections for the neutron and proton knockout. Both, for the proton and neutron knockout, the cross sections vary by many orders of magnitude. There is always a very steep rise when the nucleon energy approaches its maximal value but the cross section for the proton case is always approximately factor 10 larger than the corresponding neutron observable. The PWIA and FSI23 predictions for small T_1 values are negligible and differ very much both from the PWIAS and results taking FSI fully into account. Except for the $k1$ kinematics, we can always find an energy interval (at least on the logarithmic scale) where the group of the FSI23 lines is very close to the curve obtained with the full inclusion of FSI (when applicable). As expected, for the $k5$ and $k6$ kinematics the difference between the fully nonrelativistic and the other FSI23 results is best visible. The effects which we see for the $k7$ kinematics are magnified by the trivial differences in the allowed energy ranges.

IV. SUMMARY

Many important observables in electron induced breakup of ^{3}He are measured in kinematical regions, where a nonrelativistic approach is not applicable. Thus an approximation is needed with some relativistic features included, which can serve as a practical tool to analyze results of such experiments. One possibility is to extend the so-called FSI23 approximation (see Sec. III) which has been used since many years to include some relativistic ingredients.

In this study we added to this approach a consistent relativistic treatment of the initial 3N bound state, the relativistic single nucleon current operator, the relativistic boosted NN scattering operator and relativistic kinematics. We studied a number of electron kinematics, mostly on a quasi-elastic scattering line, in order to estimate the effects of these new relativistic ingredients. We found out that the bulk of relativistic effects comes from the relativistic kinematics. Further (consistent with kinematics) relativistic features of the calculation are less important. For the kinematics within the shaded area of Fig. 3 ($k1$, $k2$, $k3$, $k7$, $k8$), even in the neighborhood of the highest energy of the ejected nucleon, the FSI23s and the full FSI are different. Therefore the full FSI treatment is mandatory for a quantitative analysis. On top, especially for the $k7$ and $k8$ kinematics some relativistic effects are noticeable and should be included in the future analyzes of correspondingly precise data. For the kinematics $k5$ and $k6$ in the range of highest nucleon energies the relativistic effects are clearly visible, especially for neutron emission, and should be taken into account in the analysis of experimental data. Whether full FSI effects will be present there, too, cannot be answered by us right now. Nevertheless, as the first step the constructed approximate framework can be used to analyze experimental data taken at high energy and momentum transfers. In the future it should be replaced by fully relativistic calculations not available at the moment which include all FSI's along the lines of the approach applied in the 3N continuum in [20, 30].

Acknowledgments

This work was supported by the Polish Committee for Scientific Research under grant no. 2P03B00825. One of us (W.G.) would like to thank the Foundation for Polish Science

for the financial support during his stay in Kraków. The numerical calculations have been performed on the IBM Regatta p690+ of the NIC in Jülich, Germany.

---

[1] A. Nogga, A. Kievsky, H. Kamada, W. Glöckle, L.E. Marcucci, S. Rosati, M. Viviani, Phys. Rev. C**67**, 034004 (2003) and references therein.

[2] W. Glöckle, H. Witała, D. Hüber, H. Kamada,J. Golak, Phys. Rep. **274**, 107 (1996).

[3] H. Witała *et al.*, Phys. Rev. C**63**, 024007 (2001); J. Kuroś-Żołnierczuk *et al.*, Phys. Rev. C**66**, 024003 (2002).

[4] J. Golak, R. Skibiński, H. Witała, W. Glöckle, A. Nogga, H. Kamada, Phys. Rep. **415**, 89 (2005).

[5] A. Deltuva, L.P. Yuan, J. Adam Jr., P.U. Sauer, Phys. Rev. C**70**, 034004 (2004).

[6] W. Xu *et al.*, Phys. Rev. Lett. **85**, 2900 (2000).

[7] J. Golak, G. Ziemer, H. Kamada, H. Witała, W. Glöckle, Phys. Rev. C**63**, 034006 (2001); J. Golak, W. Glöckle, H. Kamada, H. Witała, R. Skibiński, A. Nogga, Phys. Rev. C**66**, 024008 (2002).

[8] J. Golak, W. Glöckle, H. Kamada, H. Witała, R. Skibiński, A. Nogga, Phys. Rev. C**65**, 044002 (2002).

[9] W. Xu *et al.*, Phys. Rev. C**67**, 012201 (2003).

[10] W. Glöckle, H. Kamada, J. Golak, A. Nogga, H. Witała, R. Skibiński, and J. Kuroś-Żołnierczuk, Acta Phys. Pol. **B32**, 3053 (2001).

[11] J. Golak, W. Glöckle, H. Kamada, H. Witała, R. Skibiński, A. Nogga, Phys. Rev. C**65**, 064004 (2002).

[12] J. Golak, R. Skibiński, H. Witała, W. Glöckle, A. Nogga, and H. Kamada, Phys. Rev. C**72**, 054005 (2005).

[13] C. Carasco *et al.*, Phys. Lett. **B559**, 41 (2003).

[14] H. Kamada, W. Glöckle, J. Golak, and Ch. Elster, Phys. Rev. C**66**, 044010 (2002).

[15] W. Glöckle, T.-S. H. Lee and F. Coester, Phys. Rev. C**33**, 709 (1986).

[16] F. Coester, Helv. Phys. Acta **38**, 7 (1965); L. Müller, Nucl. Phys. **A360**, 331 (1981); W. Glöckle, L. Müller, Phys. Rev. C**23**, 1183 (1981).

[17] J. Carlson, V. R. Pandharipande, R. Schiavilla, Phys. Rev. C**47**, 484 (1993); J. L. Forest, V. R.

Pandharipande, J. L. Friar, Phys. Rev. C**52** , 568 (1995); J. L. Forest, V. R. Pandharipande, J. Carlson, R. Schiavilla, Phys. Rev. C**52**, 576 (1995).

[18] H. Kamada, W. Glöckle, Phys. Rev. Lett. **80**, 2547 (1998).

[19] T. W. Allen, G. L. Payne, and Wayne N. Polyzou, Phys. Rev. C**62**, 054002 (2000).

[20] H. Witała, J. Golak, W. Glöckle, H. Kamada, Phys. Rev. C**71**, 054001 (2005); H. Witała, J. Golak, R. Skibiński, Phys. Lett. **B 634**, 374 (2006).

[21] S. J. Wallace, Phys. Rev. Lett. **87**, 180401 (2001).

[22] B. D. Keister and W. N. Polyzou, Phys. Rev. C**73**, 014005 (2006).

[23] W. Glöckle, *The Quantum Mechanical Few-Body Problem* (Springer-Verlag, Berlin, 1983).

[24] D. Hüber, H. Kamada, H. Witała, W. Glöckle, Few-Body Systems **16**, 127 (1994).

[25] R. Machleidt, F. Sammarruca, and Y. Song, Phys. Rev. C**53**, R1483 (1996).

[26] J. Golak, W. Glöckle, H. Kamada, H. Witała, R. Skibiński, A. Nogga, Phys.Rev. C**66**, 024008 (2002).

[27] G. Höhler, E. Pietarinen, I. Sabba-Stefanescu, F. Borkowski, G. G. Simon, V. H. Walther, and R. D. Wendling, Nucl. Phys. **B114**, 505 (1976).

[28] T. W. Donnelly, A. S. Raskin, Ann. Phys. (N.Y.) **169**, 247 (1986).

[29] J. Golak, H. Witała, R. Skibiński, W. Glöckle, A. Nogga, H. Kamada, Phys. Rev. C**70**, 034005 (2004).

[30] R. Skibiński, H. Witała, J. Golak, nucl-th/0604033.